Heliyon 6 (2020) e05133

Contents lists available at ScienceDirect

Heliyon

journal homepage: www.cell.com/heliyon

Research article

Combination of Pancreastatin inhibitor PSTi8 with metformin inhibits Fetuin-A in type 2 diabetic mice

Pragati Singh [a], Richa Garg [a,c], Umesh K. Goand [a,c], Mohammed Riyazuddin [a], Mohammad Irshad Reza [a], Anees A. Syed [a,c], Anand P. Gupta [a], Athar Husain [a,c], Jiaur R. Gayen [a,b,c,*]

[a] Pharmaceutics & Pharmacokinetics Division, CSIR-Central Drug Research Institute, Lucknow 226031, India
[b] Pharmacology Division, CSIR-Central Drug Research Institute, Lucknow 226031, India
[c] Academy of Scientific and Innovative Research (AcSIR), Ghaziabad 201002, India

ARTICLE INFO

Keywords:
Diabetes
Fetuin-A
Combination therapy
PSTi8
Metformin
Insulin resistance
Biotechnology
Biochemistry
Molecular biology
Pharmacology
Endocrinology
Metabolism
Metabolic disorder
Pharmaceutical science

ABSTRACT

In the preceding study, we delineated that high-fat diet (HFD) consumption in mice increases the circulatory level of pancreastatin (PST), which additionally enhances the free fatty acid (FFA) concentration in circulation. Consequently, the aggravated FFA activates Fetuin-A, which facilitates hepatic lipid accumulation, insulin resistance (IR), and culminates in type 2 diabetes (T2D). Metformin (Met) is a widely known first-line drug for the treatment of T2D. We previously unveiled PSTi8, an inhibitor of PST, comprising antidiabetic property. Hence, we hypothesized that combination therapy of Met and PSTi8, at reduced therapeutic doses, would mitigate HFD-induced IR by inhibiting hepatic Fetuin-A in mice model of T2D. C57BL/6 mice were fed HFD for 12 weeks, followed by treatment with Met, PSTi8, and its combination for 10 days. Glucose and insulin tolerance tests were conducted. Circulatory levels of PST, Fetuin-A, and lipid markers were determined. Also, the mRNA and protein expression of Fetuin-A was assessed by qPCR, western blotting, and immunofluorescence. Moreover, the energy expenditure was measured by comprehensive laboratory animal monitoring system (CLAMS). Combination therapy displayed improved PST, Fetuin-A, and lipid profile in plasma. We also found reduced hepatic Fetuin-A, which reduced inhibitory phosphorylation of IRS and increased phosphorylation of AKT. Consequently, ameliorated hepatic lipogenesis, gluconeogenesis, and inflammation. Also, combination treatment attenuated Fetuin-A expression, lipid accumulation, and glucose production in palmitate-induced HepG2 cells. Altogether current study promulgates the beneficial effect of combination therapy of Met and PSTi8 (comparable to alone higher therapeutic doses) to ameliorate Fetuin-A activation, hepatic lipid accumulation, insulin resistance, and associated progressive pathophysiological alterations in T2D.

1. Introduction

Type 2 diabetes (T2D) manifests diminished insulin production and increased peripheral insulin resistance (IR) (Arulmozhi et al., 2008), violating the stringent regulation of hepatic carbohydrate and lipid metabolism (Olefsky, 1990; Reaven, 1988). Worldwide 463 million people had diabetes in 2019, and this number is expected to rise to 578 million in 2030 and 700 million by 2045 (Saeedi et al., 2019; Un Nisa and Reza, 2019). The liver has exquisite management to regulate fatty acid synthesis and triglyceride production. For this reason, the liver probably is considered as the primary organ wherefrom IR emerges and further leads to progression into muscle and adipose tissue (Seppala-Lindroos et al., 2002). A high-fat diet (HFD) fed murine model is a well-established model to investigate the interrelationship between IR and T2D in humans (Nath et al., 2017). Pancreastatin (PST) plays important role in lipid metabolism. PST enhances free fatty acids in circulation (Bandyopadhyay et al., 2015). Also, it has been reported that increased free fatty acids are the major culprit, plays pivotal function in activation of Fetuin-A, which is a well-known factor for 2the development of IR (Stefan et al., 2008). According to the American Diabetes Association and the European Association for the Study of Diabetes, first-line therapy for diabetes treatment is metformin (Met). Elevated concentrations of Met has been allegedly believed to be the cause of gastrointestinal side-effects (Rena et al., 2017). Hence there is an urgent need for combination therapy with

* Corresponding author.
E-mail address: jr.gayen@cdri.res.in (J.R. Gayen).

https://doi.org/10.1016/j.heliyon.2020.e05133
Received 14 September 2020; Received in revised form 20 September 2020; Accepted 28 September 2020

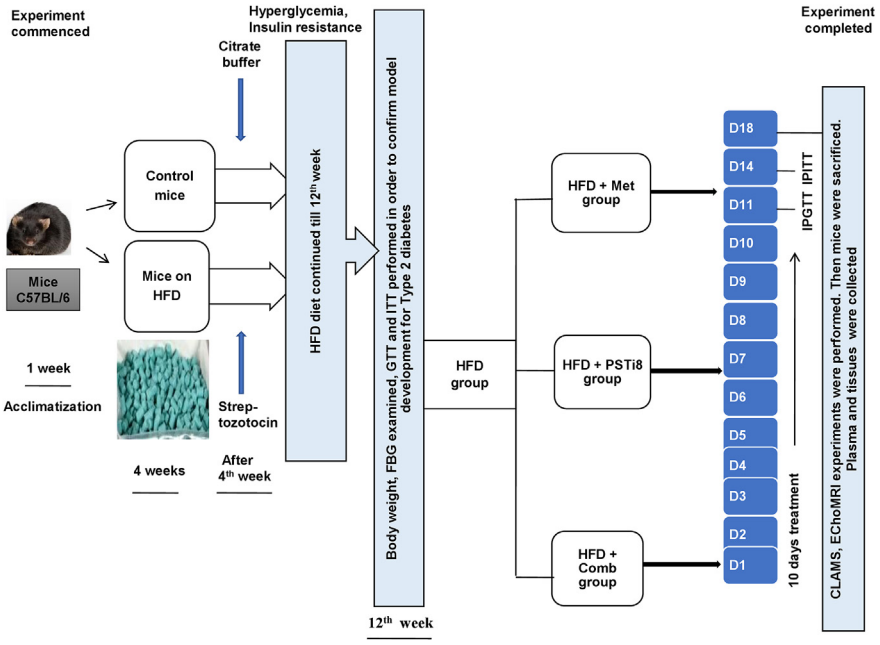

Figure 1. Experimental design of HFD model development and therapeutic intervention.

Met at lower doses to preserve glycemic control. PSTi8, an emerging peptide, reported to have antidiabetic effects by inhibiting PST derived IR and inflammation (Bandyopadhyay et al., 2015; Funakoshi et al., 1990; Hossain et al., 2018; Valicherla et al., 2019). Chronic treatment of PSTi8 improved glycemic control, glucose tolerance, and IR, as stated in previous research (Valicherla et al., 2019).

In the current work, we aimed to decipher that if combination therapy of Met and PSTi8, at reduced therapeutic doses, would be able to attenuate Fetuin-A mediated IR and subsequent pathologies in the liver, underpinning T2D in HFD model.

2. Materials and methods

2.1. Materials

Peptide PSTi8 (PEGKGEQEHSQQKEEEEEMAV-amide, synthesized by Life Tein LLC, USA), 1,1-DimethylbiguanideHCl (Metformin) purchased from Alfa Aesar. Low glucose and without glucose Dulbecco modified eagle's medium, sodium lactate, sodium pyruvate, glucose, Insulin, TRIzol reagent, phosphate-buffered saline, glycogen, anthrone, Oil Red O, Nile Red, trypsin-EDTA, and antibiotic-antimycotics solution were purchased from Sigma Aldrich, St. Louis, USA. Streptozotocin was procured from Enzo life sciences, New York, USA. High capacity cDNA Reverse Transcription kit, amplex™ red glucose/glucose oxidase assay kit, DyNAmo Color Flash SYBR Green qPCR Kit, Immobilon Western Chemiluminescent HRP substrate was purchased from Thermo Fisher Scientific, Waltham, USA. Primers for real time-PCR were purchased from Eurofins Scientific, Luxembourg. HFD (60% of calories from fat, cat. No. D12492) was obtained from research diets, Inc, USA. Mouse pancreastatin ELISA kit was obtained from MyBioSource, San Diego, USA. Primary antibodies phospho-AKT (Ser473) (4058S), pan AKT (4691S), phospho-IRS (Ser307) (2381P), IRS-1(2382S), anti-mouse IgG, HRP-linked secondary antibody (7076S) were purchased from Cell Signalling Technology, Denvers. Goat anti-rabbit IgG HRP linked secondary antibody was (HAF008) purchased from R&D systems. NEFA ELISA kit (E-BC-K013-M) was purchased from Elabscience Biotechnology. Fetuin-A (SC-133146) obtained from Santa Cruz Biotechnology, Dallas, USA. GAPDH (MAB374) was purchased from Merkmillipore, Burlington, USA. Mouse Alexa Fluor 594 was procured from Invitrogen, Waltham, USA.

2.2. Animals

HFD fed murine model was developed using 7–8 weeks old male C57BL/6 mice (20 ± 2 g). Mice were provided by the Laboratory Animal Facility of CSIR-Central Drug Research Institute (CDRI), Lucknow, India. Mice were continued with *ad libitum* standard chow diet (SD) and were kept in polypropylene cages with consistent 12-h light/dark cycle at constant temperature (22–25 °C) with relative humidity 60–70% in the animal house room for acclimatization. All the animal studies were performed as per the approved protocol (IAEC/2018/F-26) of the institutional animal ethics committee of CSIR-CDRI.

2.3. Experimental design and treatment protocol

We have briefed the experimental design in Figure 1. At the commencement of the experiment, mice were categorized into the Control group, fed with a standard diet (SD) and HFD group, fed with HFD. After 4 weeks duration, HFD group mice were administered with a single dose of streptozotocin (100 mg/kg) (Luo et al., 1998) intraperitoneally, and the Control group was exposed to vehicle (0.1 M citrate buffer, pH 4.5). Furthermore, mice were kept on their respective diets for the next 12 weeks. At 12th week, HFD group mice were randomly divided into four groups with 6 mice in each group: group first- HFD, group second- HFD + Met, group third- HFD + PSTi8, group fourth- HFD + Comb. Following preliminary study regarding dose selection for combination of Met and PSTi8, Intraperitoneal glucose tolerance test (IPGTT) and intraperitoneal insulin tolerance test (IPITT) were performed with acute drug treatment of Met (300 mg/kg) (Calixto et al., 2013; Salomäki et al., 2013), PSTi8 (5 mg/kg) (Hossain et al., 2018) and Comb (Met 150 mg/kg + PSTi8 2.5 mg/kg) to determine the development of glucose intolerance, reduced insulin sensitivity and simultaneously acute effect of treatments on emerging pathophysiology. After successful confirmation of the development of hyperglycemia, glucose intolerance and insulin insensitivity

Table 1. Primers used in the study.

Gene	Primer Sequence
mSrebp-1c (Forward)	GGTTTTGAACGACATCGAAGA
mSrebp-1c (Reverse)	CGGGAAGTCACTGTCTTGGT
mFas (Forward)	CGGAAACTTCAGGAAATGTCC
mFas (Reverse)	TCAGAGACGTGTCACTCCTGG
mChrebp (Forward)	CTGGGGACCTAAACAGGAGC
mChrebp (Reverse)	GAAGCCACCCTATAGCTCCC
mCpt-1α (Forward)	GACTCCGCTCGCTCATTC
mCpt-1α (Reverse)	TCTGCCATCTTGAGTGGTGA
mPgc-1α (Forward)	AGCCGTGACCACTGACAACGAG
mPgc-1α (Reverse)	CTGCATGGTTCTGAGTGCTAAG
mTnf-α (Forward)	TCTTCTCATTCCTGCTTGTGG
mTnf-α (Reverse)	GGTCTGGGCCATAGAACTGA
mIl-6 (Forward)	GCTACCAAACTGGATATAATCAGGA
mIl-6 (Reverse)	CCAGGTAGCTATGGTACTCCAGAA
mIl-1β (Forward)	TGTAATGAAAGACGGCACACC
mIl-1β (Reverse)	TCTTCTTTGGGTATTGCTTGG
mPepck (Forward)	ATGTGTGGGCGATGACATT
mPepck (Reverse)	AACCCGTTTTCTGGGTTGAT
mG6pase (Forward)	CATGGGCGCAGCAGGTGTATACT
mG6pase (Reverse)	CAAGGTAGATCCGGGACAGACAG
mGapdh (Forwad)	GTGTCCGTCGTGGATCTGA
mGapdh (Reverse)	CCTGCTTCACCACCTTCTTG
mβactin (Forward)	CCTCACCCTCCCAAAAGC
mβactin (Reverse)	GTGGACTCAGGGCATGGA

in response to glucose challenge, mice were treated with Met (300 mg/kg), PSTi8 (2 mg/kg) and combination (Met150 mg/kg + PSTi8 1 mg/kg) for 10 days consecutively (Hossain et al., 2018). To determine the effect of chronic combination treatment IPGTT, IPITT was performed. Furthermore, mice were inspected in CLAMS and EchoMRI. After that, mice were sacrificed, blood plasma was collected to estimate lipid parameters, hormones, and hepatokine levels. Tissues were collected for histopathological examination, glycogen measurement, and expression studies.

Mice were divided into control group (Control), fed with a standard diet (SD) and HFD group, fed with HFD. After 4 weeks of feeding, HFD mice were administered with a single dose of streptozotocin (100 mg/kg, ip), and the Control group was exposed to vehicle (0.1 M citrate buffer, pH 4.5). At 12^{th} week, HFD group mice were randomly divided into four groups (n = 6): group first- HFD, group second- HFD + Met, group third- HFD + PSTi8, group fourth- HFD + Comb. Intraperitoneal glucose tolerance test (IPGTT) and intraperitoneal insulin tolerance test (IPITT) were performed with acute drug treatment of Met (300 mg/kg), PSTi8 (5 mg/kg) and Comb (Met 150 mg/kg + PSTi8 2.5 mg/kg). After successful confirmation of the development of hyperglycemia and insulin resistance mice were treated with Met (300 mg/kg), PSTi8 (2 mg/kg) and combination (Met150 mg/kg + PSTi8 1 mg/kg) for 10 days consecutively. Subsequently, to determine the effect of chronic combination treatment, IPGTT, IPITT were performed. Furthermore, mice were inspected in CLAMS and EchoMRI. Thereafter mice were sacrificed, blood plasma was collected to estimate lipid parameters, hormones, and hepatokine levels, and tissues were collected for histopathological examination, glycogen measurement, and expression studies.

2.4. Intraperitoneal glucose and insulin tolerance test

IPGTT and IPITT were performed in mice, fasted for 6 h. We conducted preliminary study regarding selection of doses for combination of Met and PSTi8 in HFD mice model. Control and HFD group mice received 0.9 % saline. Different combinations which were used are Met 75 mg/kg + PSTi8 1.25 mg/kg, Met 75 mg/kg + PSTi8 2.5 mg/kg, Met 150 mg/kg + PSTi8 1.25 mg/kg, Met 150 mg/kg + PSTi8 2.5 mg/kg. Next, selected combination of Met and PSTi8 were used for further IPGTT and IPITT experiments in HFD induced diabetic mice. For IPGTT, HFD + Met group received Met (300 mg/kg), HFD + PSTi8 group received PSTi8 (5 mg/kg) (acute) or PSTi8 2 mg/kg (chronic) and HFD + Comb group received Met 150 mg/kg + PSTi8 2.5 mg/kg (acute) or Met 150 mg/kg + PSTi8 1 mg/kg (chronic), before 30 min of glucose or insulin exposure. Blood glucose was measured at 0, 15, 30, 60, 90, 120 min after administration of glucose (1 g/kg) and insulin (0.75 IU/kg) challenge during IPGTT and IPITT respectively. Area under curve (AUC) was calculated by using graphpad prism software. HOMA-IR was calculated according to the formula [fasting plasma glucose (mmol/L) x fasting plasma insulin (uU/mL)/22.5] (Ables et al., 2012).

2.5. Body composition analysis

Body composition (lean mass and fat mass) analysis of animals was done by EchoMRI body composition analyzer (E26-226-RM EchoMRI LLC, USA). It works through radio frequency pulses applied at a distinct static magnetic field. The body composition of each animal was measured by placing it in a plastic cylinder (4.5 cm diameter) with restricted movement (Gupta et al., 2019).

2.6. Energy expenditure measurements

Comprehensive lab animal monitoring system (Oxymax-CLAMS), Columbus, USA, was utilized to gauge the energy homeostasis and evaluation of metabolic parameters in animals. The experiment was under optimum temperature (22–25 °C) with 12 h/12 h light-dark cycle. CLAMS system was calibrated with the standard ratio of O_2, CO_2, and balanced nitrogen gas mixture before initiation of the experiment. In this system, an individual chamber facility for animals was provided for the detection of O_2 consumption CO_2 release, heat production, and RER.

2.7. Estimation of plasma PST and Fetuin-A level

The level of PST and Fetuin-A were estimated in plasma using Mouse Pancreastatin (MBS267929) and Fetuin-A (E-EL-M2459) ELISA kits, respectively, following the manufacturer's instruction.

2.8. Measurement of plasma lipids and insulin level

For the detection of plasma parameters, mice fasted for 6 h, and blood were withdrawn from the ophthalmic vein before sacrifice. Detection of plasma levels of HDL by using kits such as High-density Lipoprotein Cholesterol (HDL-C) (E-BC-K221), LDL by Low-density Lipoprotein Cholesterol (LDL-C) (E-BC-K205) and triglycerides were measured by triglyceride Colorimetric assay Kit (E-BC-K238). The level of NEFA was estimated in plasma by Non-esterified Free Fatty Acids (NEFA) Colorimetric Assay Kit (E-BC-K013-M). Also, plasma insulin was also determined by the Mouse Insulin ELISA kit (E-EL-M1382).

2.9. Evaluation of glycogen content in liver

Glycogen content was determined by dissolving liver tissue in hot KOH (30%). Liver tissue was then precipitated and centrifuged at 5000 rpm for 12 min. After centrifugation, the pellet was dissolved in 5 mL water and then mixed with anthrone reagent. Glycogen concentration was detected by absorbance measured at 620 nm (Gayen et al., 2009).

2.10. Morphological analysis of liver

Liver tissues were stored in neutral buffer formalin for fixation, immediately after sacrifice. Formalin-fixed tissues were dehydrated by the use of different concentrations of ethanol (70%, 90%, and 100%) and treated with xylene (two treatments). Paraffin-embedded tissue sections were deparaffinized in xylene and rehydrated with ethanol percentage 100%, 70%, 50%,

and stained with H & E stain. Images were captured at 20 X magnification (Leica DM-5000). Lipid accumulation was calculated in terms of steatosis and hepatic ballooning score, as previously described (Syed et al., 2020).

2.11. Extraction of RNA and quantitative real-time PCR

TRIzol procedure was used to extract total RNA from liver tissue and quantified by NanoDrop-2000 Spectrophotometers, Thermo Fisher Scientific, Waltham, USA. After RNA isolation, it was reverse transcribed into cDNA using the high capacity cDNA Reverse Transcription kit and SureCycler 8800 (Agilent Technologies, USA). Reaction conditions for cDNA preparation were 25 °C for 10 min; 37 °C for 120 min; 85 °C for 5 min; hold at 4 °C (Gupta et al., 2019). Further real-time PCR (RT-PCR) was conducted using DyNAmo Color Flash SYBR Green qPCR Kit, by RT-PCR LightCycler 480 Instrument II (Roche Life Science). Reaction conditions were programmed as initial incubation at 95 °C for 7 s with following 40 cycles comprising 95 °C for 10 s, 60 °C for 15 s and 72 °C for 15 s. For data analysis, delta Ct values were used to calculate relative mRNA expression. Primers used in the present study are listed in Table 1.

2.12. Western blotting

Liver tissue was homogenized in lysis buffer containing protease inhibitor cocktail and phosphatase inhibitor cocktail at 4 °C. Proteins were separated by 10% SDS-PAGE at constant voltage 100 volts for 2.5 h. PVDF membrane was used to transfer proteins and blocked with 5% (w/v) non-fat milk powder in PBST for 1 h. PVDF membrane was immunoblotted with primary antibodies, including Fetuin-A, phospho-Insulin receptor substrate -1 (pIRS-1) (Ser307), IRS-1, phospho-protein kinase B (p-AKT) (Ser473), Pan AKT, glyceraldehyde-3-phosphate dehydrogenase (GAPDH) overnight at 4 °C. Immobilon Western Chemiluminescent HRP substrate was used to visualize bands in myECL imager of Thermo Fischer Scientific Waltham, USA. Recognized signals were normalized with their corresponding controls and analyzed by quantitative densitometry with the use of Image J software.

2.13. Cell culture studies

HepG2 cells (ATCC, Manasses, VA, USA), were cultured in low glucose Dulbecco's Modified Eagle's Medium (LGDMEM) with 10 % FBS, antibiotics (L-Glutamine-Penicillin-Streptomycin solution) and allowed to grow in a humidified atmosphere of 5 % CO_2 at 37 °C.

2.14. Glucose production assay

For glucose production assay, HepG2 cells were seeded in 6 well culture plates at cell density 0.3×10^5 in each well. Then cells were treated with or without Palmitate (Pal: 250 uM) (Gao et al., 2010). For preliminary screening of combination dose selections cells were treated with different combinations of Met and PSTi8 as Met 25 μM + PSti8 50 nM, Met 25 μM + PSti8 100 nM, Met 50 μM + PSTi8 50 nM, Met 50 μM + PSTi8 100 nM. Furthermore we performed individual study with Met (100 μM) (Kim et al., 2010), PSTi8 (200 nM) (Gupta et al., 2019) and selected combination of Met 50 uM with PSTi8 100 nM for 24 h followed by insulin (100 nM), treatment for last 20 min. Glucose production media (2 ml/well, DMEM without glucose supplemented with 20 mM sodium lactate and 2 mM sodium pyruvate) was added to the wells followed by 3–4 h incubation after giving two times PBS wash. After incubation, cells and media were collected and used for protein estimation and glucose determination (Amplex red glucose assay kit) (Cao et al., 2014), respectively.

2.15. Glucose uptake assay

For glucose uptake assay, HepG2 cells (seeded in 96 well culture plate) were induced with Pal (250 μM) for 24 h and treated with different combinations of Met and PSTi8. These combinations were Met 25 μM + PSti8 50 nM, Met 25 μM + PSti8 100 nM, Met 50 μM + PSTi8 50 nM, Met 50 μM + PSTi8 100 nM. We followed the glucose uptake procedure according to instructions provided in kit manual (Sigma Glucose Uptake Assay kit, cat- MAK0083).

2.16. Nile Red and oil red O staining to detect lipid accumulation

For preliminary study of Met and PSTi8 combination dose selection in Pal (250 μM) induced insulin resistant HepG2 cells, different combinations of Met and PSTi8 were used to detect oil droplet accumulation. These combinations were Met 25 μM + PSTi8 50 nM, Met 25 μM + PSTi8 100 nM, Met 50 μM + PSTi8 50 nM, Met 50 μM + PSTi8 100 nM. Following detection of best combination doses of Met and PSTi8 we performed separate study to verify the effects of Met and PSTi8 selected combination on ectopic lipid accumulation, we have determined lipid accumulation in HepG2 cells in the presence of Pal treatment 250 uM (Xiao et al., 2019). After 80–90 % confluency, media was changed and treated with Met 100 uM, PSTi8 200 nM, Combination (Met 50 uM + PSTi8 100 nM) in insulin-resistant conditions for 24 h. After treatment duration, the media was removed, washed twice with PBS (phosphate--buffered saline). For Nile Red, cells were incubated with Nile Red stain, washed with PBS, and observed under a fluorescence microscope (Leica) for imaging. Similarly, for Oil Red O, washed cells were incubated with Oil Red O stain (0.36 % in 60 % isopropanol), washed with PBS, dried, and absorbance (540 nm) was measured in the presence of isopropanol (Benarbia et al., 2013).

2.17. Immunofluorescence

To unravel the effect of combination therapy on Fetuin-A expression in Pal exposed HepG2 cells, we performed immunofluorescence as previously established in our lab (Syed et al., 2020). HepG2 cells were grown in 96-well plate. After 50–60 % confluency, media was changed and treated with Met 100 uM, PSTi8 200 nM, and combination (Met 50 uM + PSTi8 100 nM) in insulin-resistant conditions for 24 h. Cells were washed three times with PBS and then fixed and permeabilized with cold methanol for 20 min. Methanol was washed with PBS three times, and cells were blocked in 5% BSA for 2 h. Then, cells were washed with PBS 5 times and incubated overnight with primary antibody anti-Fetuin-A, followed by incubation with species-specific Alexa Fluor 594 for 2 h. Further, cells were washed with PBS 5 times, DAPI was added, and examined under a fluorescence microscope (Leica).

2.18. Statistical analysis

Results presented in this study were expressed as mean ± SEM, and GraphPad prism software, San Diego, CA, USA, was used to analyze the data. We performed statistical analyses with the use of Student's t-tests, one or two-way ANOVA followed by Bonferroni posttest wherever required.

3. Results

3.1. Selection of best possible combination of Met and PSTi8 and appraisal of murine model development of T2D

Glucose release assay (Figure 2A), glucose uptake assay (Figure 2B), Oil Red O staining (Figure 2C) experiments in presence of Pal (250 μM) induction in HepG2 cells, revealed that Met 50 μM and PSTi8 100 nM combination is most optimal among other combinations for *in-vitro* experiments. Furthermore we also performed GTT in HFD fed diabetic mice model to detect best combination of Met and PSTi8 in *in-vivo* experiments (Figure 2D–E). Results revealed that Met 150 mg/kg with PSTi8 2.5 mg/kg significantly reduced glucose intolerance among other combinations. Then we further used this optimized combination for additional *in-vivo* experiments. Additionally, we detected alterations in body weight (Figure 2F) and FBG (Figure 2G) before and after treatment. There was

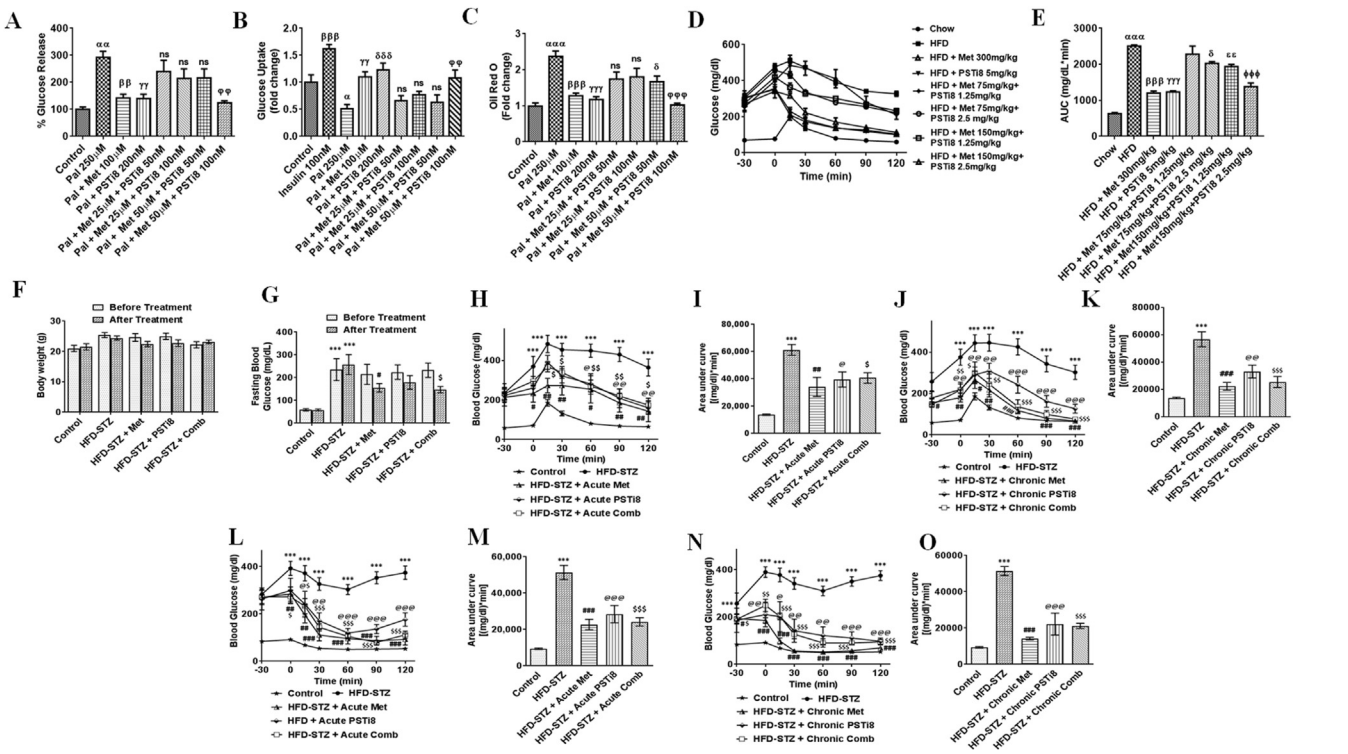

Figure 2. Dose selection study for combination of Met and PSTi8 with different doses of Met and PSTi8, HFD mouse model development and effect of combination therapy on glucose intolerance and reduced insulin sensitivity. (A) Glucose production assay to detect glucose production in Pal (250 μM) induced insulin resistant HepG2 cells (24 h) to select best combination of Met and PSTi8 (n = 3). (B) Glucose uptake assay to detect glucose uptake in Pal (250 μM) induced HepG2 cells (24 h) to select effective combination of Met and PSTi8 (n = 6). (C) Oil Red O staining in Pal (250 μM) induced HepG2 cells (24 h) to choose best possible combination of Met and PSTi8 (n = 5). (D) IPGTT with different combinations of Met and PSTi8 and its relevant (E) AUC. (F) Body weight and (G) fasting blood glucose measured before and after treatment. GTT and ITT were performed with optimized combination of Met and PSTi8 as (H) Acute IPGTT with relevant (I) AUC with acute treatment of Met 300 mg/kg, PSTi8 5 mg/kg and Combination Met 150 mg/kg + PSTi8 2.5 mg/kg including glucose 1 g/kg and (J) chronic IPGTT with related (K) AUC with chronic treatment of Met 300 mg/kg, PSTi8 2 mg/kg, and Combination Met 150 mg/kg + PSTi8 1 mg/kg were conducted (n = 6). We also performed (L) Acute IPITT related (M) AUC, with acute treatment of Met 300 mg/kg, PSTi8 5 mg/kg and Combination Met 150 mg/kg + PSTi8 2.5 mg/kg, including insulin 0.75 IU/kg (N) chronic IPITT and its corresponding (O) AUC with chronic treatment of Met 300 mg/kg, PSTi8 2 mg/kg, and Combination Met 150 mg/kg + PSTi8 1 mg/kg and insulin 0.75 IU/kg (n = 6). Results are shown as means ± SEM. Significance in group comparisons for (A) presented as α, Control vs Pal; β, Pal vs Pal + Met; γ, Pal vs Pal + PSTi8; Φ, Pal vs Pal + Met 50 μM + PSTi8 100 nM. Significance values depicted as $^{\alpha,\beta,\gamma,\phi}p<0.05$; $^{\alpha\alpha,\beta\beta,\gamma\gamma,\phi\phi}p<0.01$; $^{\alpha\alpha\alpha,\beta\beta\beta,\gamma\gamma\gamma,\phi\phi\phi}p<0.001$. For (B) significance in group comparisons followed as α, Control vs Pal; β, Pal vs Ins; γ, Pal + Met; δ Pal vs Pal + PSTi8; Φ, Pal vs Pal + Met 50 μM + PSTi8 100 nM. Significance values depicted as $^{\alpha,\beta,\gamma,\delta,\phi}p<0.05$; $^{\alpha\alpha,\beta\beta,\gamma\gamma,\delta\delta,\phi\phi}p<0.01$; $^{\alpha\alpha\alpha,\beta\beta\beta,\gamma\gamma\gamma,\delta\delta\delta,\phi\phi\phi}p<0.001$. For (C) Results are shown as means ± SEM (n = 5). Significance in group comparisons represented as α, Control vs Pal; β, Pal vs Pal + Met; γ, Pal + PSTi8; δ, Pal vs Pal + Met 50 μM + PSTi8 50 nM; Φ, Pal vs Pal + Met 50 μM + PSTi8 100 nM. Significance values depicted as $^{\alpha,\beta,\gamma,\delta,\phi}p<0.05$; $^{\alpha\alpha,\beta\beta,\gamma\gamma,\delta\delta,\phi\phi}p<0.01$; $^{\alpha\alpha\alpha,\beta\beta\beta,\gamma\gamma\gamma,\delta\delta\delta,\phi\phi\phi}p<0.001$. ns, non significant. For (E) Results are shown as means ± SEM (n = 6). Significance in group comparisons represented as α, Control vs HFD; β, HFD vs HFD + Met 300 mg/kg; Met; γ, HFD vs HFD + PSTi8; δ, HFD vs HFD + Met 150 mg/kg + PSTi8 1.25 mg/kg; ϕ, HFD vs HFD + Met 150 mg/kg + PSTi8 2.5 mg/kg. Significance values expressed as $^{\alpha,\beta,\gamma,\delta,\varepsilon,\phi}p<0.05$; $^{\alpha\alpha,\beta\beta,\gamma\gamma,\delta\delta,\varepsilon\varepsilon,\phi\phi}p<0.01$; $^{\alpha\alpha\alpha,\beta\beta\beta,\gamma\gamma\gamma,\delta\delta\delta,\varepsilon\varepsilon\varepsilon,\phi\phi\phi}p<0.001$. For (F–O) significance in group comparisons represented as *, Control vs HFD; #, HFD vs HFD + Met; @, HFD vs HFD + PSTi8; $, HFD vs HFD + Comb. Significance values expressed as $^{*,\ \#,\ @,\ \$}p < 0.05$; $^{**,\ \#\#,\ @@,\ \$\$}p < 0.01$; $^{***,\ \#\#\#,\ @@@,\ \$\$\$}p < 0.001$.

not much distinct variability in body weight, while FBG was more significantly reduced in HFD + Comb group. We performed intraperitoneal tolerance tests in response to glucose and insulin challenge to assess the decisive role of lipid overabundance on insulin sensitivity and insulin action on glucose disposal. During IPGTT, we found an increased glucose expedition in the HFD group while in HFD + Comb group, elevated blood glucose started to reduce after 30 min during acute (Figure 2H) and more significantly during chronic treatment (Figure 2J). Corresponding AUC for IPGTT with acute (Figure 2I) and chronic treatment (Figure 2K) also demonstrated significant glucose intolerance developed in HFD and improved in co-administered Met and PSTi8 treatment groups. IPITT was also performed to examine insulin influence to mitigate blood glucose, and we found diminished insulin action in HFD group while improved significantly after 15 min and continued to maintain the basal level in HFD + Comb group with both acute (Figure 2L) and chronic (Figure 2N) treatment conditions. AUC analysis relevant to IPITT for acute treatment was shown in Figure 2M and chronic treatment in Figure 2O. Hence these results suggested that combination treatment possibly be able to prevent the development of IR and improve insulin response.

3.2. Effect of combination therapy in restoring PST induced free fatty acids and Fetuin-A

It has been speculated that PST enhances NEFA in circulation, which may further result in hepatic Fetuin-A activation and, subsequently, IR. Hence, we detected plasma PST, NFFA, and Fetuin-A level in plasma and observed significantly increased plasma PST (Figure 3A), NFFA (Figure 3B), Fetuin-A (Figure 3C) in HFD group and it was found to be significantly reduced by combination therapy. We have found increased relative mRNA (Figure 3D) and protein expression (Figure 3E) of Fetuin-A in HFD mice liver, while its expression was significantly reduced by combination therapy. We have also found increased fluorescence intensity of Fetuin-A in pal-induced HepG2 cells (Figure 3F, G). On the contrary, Combination therapy significantly inhibited Fetuin-A in pal-induced HepG2 cells, as it showed decreased fluorescence intensity in pal-induced HepG2 cells. Hence combination therapy of Met and PSTi8 effectively ameliorated PST induced adverse effects by inhibiting Fetuin-A.

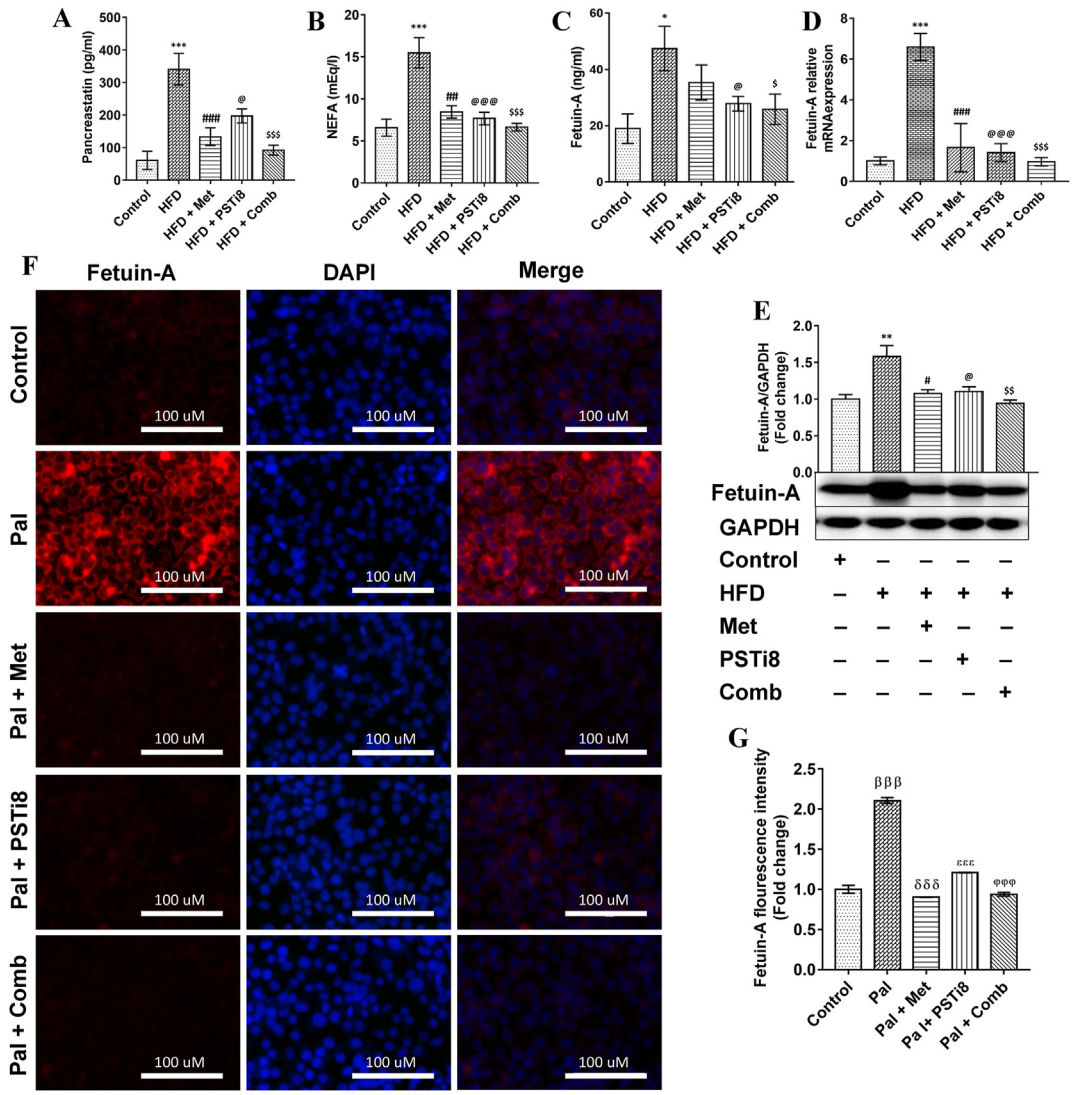

Figure 3. Effects of combination therapy on PST induced Free fatty acids and Fetuin-A. (A) Plasma levels of PST (B) NEFA and (C) Fetuin-A. (D) Real-Time PCR results showing relative mRNA expression of Fetuin-A in the liver (n = 6). (E) Immunoblotting of Fetuin-A in the liver. We further confirmed the enhanced Fetuin-A in pal-induced insulin-resistant HepG2 cells by immunofluorescence (F) and (G) quantified (Image J). Data values are shown as means ± SEM. Comparative significance for A–C, E and F represented as *, Control vs HFD; #, HFD vs HFD + Met; @, HFD vs HFD + PSTi8; $, HFD vs HFD + Comb. $^{*,\#,@,\$}p < 0.05$; $^{**,\#\#,@@,\$\$}p < 0.01$; $^{***,\#\#\#,@@@,\$\$\$}p < 0.001$. For G significance comparison represented as β, Control vs Pal; δ, Pal vs Pal + Met, ε, Pal vs Pal + PSTi8; Φ, Pal vs Pal + Comb. Significance values depicted as $^{\beta,\delta,\varepsilon,\Phi}p<0.05$; $^{\beta\beta,\delta\delta,\varepsilon\varepsilon,\Phi\Phi}p<0.01$; $^{\beta\beta\beta,\delta\delta\delta,\varepsilon\varepsilon\varepsilon,\Phi\Phi\Phi}p<0.001$.

3.3. Combination therapy ameliorated Fetuin-A induced insulin resistance by activated insulin signaling

In the present study, we utilized the HFD model to detect the effect of combination therapy in ameliorating Fetuin-A mediated IR. We found increased fasting plasma insulin levels in HFD group (Figure 4A) and significantly reduced plasma insulin concentrations in the HFD + Comb group. We calculated the homeostasis model assessment of IR (HOMA-IR) (Figure 4B), an essential determinant for insulin sensitivity. We found increased IR in the HFD group, whereas combination therapy significantly improved insulin sensitivity. Moreover, this increased insulin sensitivity may lead to increased hepatic glycogen production. Therefore, we estimated hepatic glycogen content (Figure 4C) and found that combination therapy significantly increased glycogen content equivalent to individual therapies of Met and PSTi8. Likewise, we have measured glucose production in Pal induced insulin-resistant HepG2 cells (Figure 4D). We found a significant increase in glucose production due to Pal induced IR in HepG2 cells and reduction in glucose release in Pal + Comb group significantly. It has been figured out so far that AKTand IRS-1 are important downstream elements of insulin signaling (Guo, 2014), and IR may cause perturbations in their phosphorylation pattern. Therefore, we investigated whether combination therapy may activate insulin signaling by preventing insulin-resistant conditions in the HFD model. We found that IRS-1 phosphorylation (Ser-307) was increased (Figure 4E) and phosphorylation of AKT (Ser-473) was decreased (Figure 4F) in HFD group while IRS phosphorylation was found to be decreased markedly (Figure 4E) and AKT phosphorylation was increased significantly (Figure 4F) in HFD + Comb group. Thus, combination therapy efficiently improved insulin sensitivity, thereby improved glycogen production in the liver and also ameliorated glucose production in insulin-resistant HepG2 cells.

3.4. Combination therapy imparts improvement in lipid homeostasis

As we hypothesized that excess lipid load is the substantial miscreant in the HFD model to cause further pathological conditions; accordingly, we investigated herein plasma lipid profile, fat mass percent, ectopic lipid accumulation in the liver along with lipid deposition in insulin-resistant HepG2 cells. We found decreased HDL-C (Figure 5A) levels in

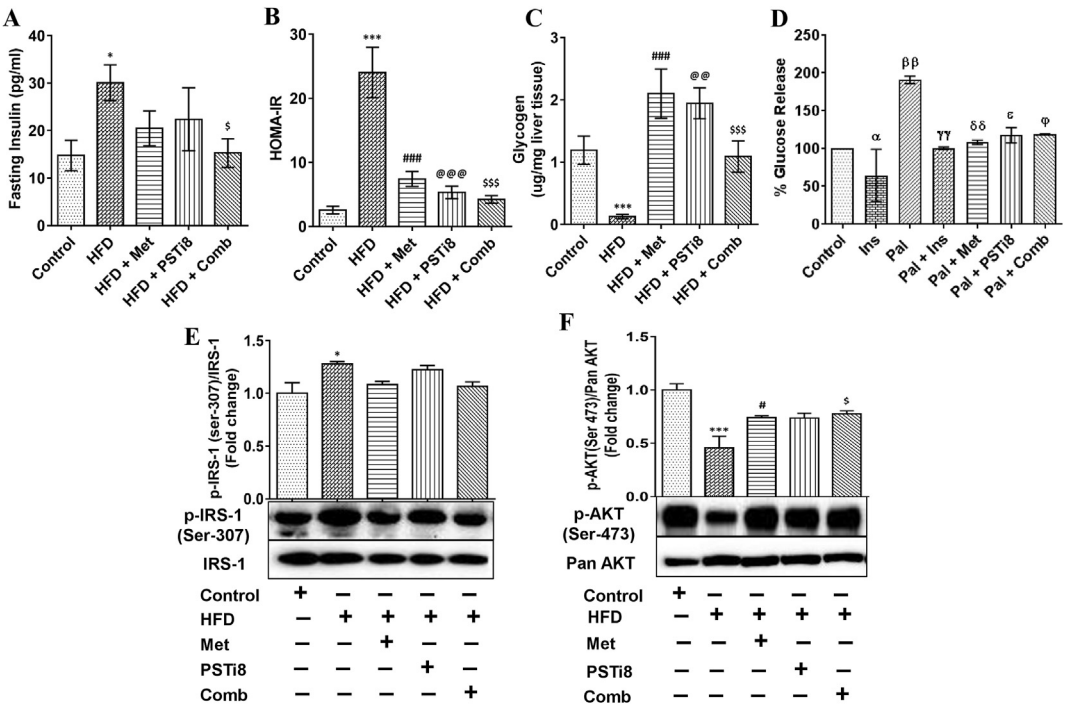

Figure 4. Combination therapy ameliorated Fetuin-A induced insulin resistance. (A) Fasting plasma insulin was detected after 6 h fasting (n = 6). (B) Analyzed HOMA-IR to determine insulin sensitivity (n = 6). (C) To envisage the results of insulin sensitivity, hepatic glycogen content was determined (n = 6). (D) Glucose production in insulin-resistant HepG2 cells (n = 3, with 2 independent experiments). To deduce the effect of combination therapy on insulin signaling, we detected the expression of (E) phospho-IRS-1 (Ser-307)/IRS-1 and (F) phospho-Akt (Ser-473)/pan-Akt (n = 3). Data values are shown as means ± SEM. Comparative significance for A–C, E and F represented as *, Control vs HFD; #, HFD vs HFD + Met; @, HFD vs HFD + PSTi8; $, HFD vs HFD + Comb. $^{*,\#,@,\$}p < 0.05$; $^{**,\#\#,@@,\$\$}p < 0.01$; $^{***,\#\#\#,@@@,\$\$\$}p < 0.001$. For D significance comparison represented as α, Pal vs Ins; β, Control vs Pal; γ, Pal vs Pal + Ins; δ, Pal vs Pal + Met, ε, Pal vs Pal + PSTi8; Φ, Pal vs Pal + Comb. Significance values depicted as $^{\alpha,\beta,\gamma,\delta,\varepsilon,\phi}p<0.05$; $^{\alpha\alpha,\beta\beta,\gamma\gamma,\delta\delta,\varepsilon\varepsilon,\phi\phi}p<0.01$; $^{\alpha\alpha\alpha,\beta\beta\beta,\gamma\gamma\gamma,\delta\delta\delta,\varepsilon\varepsilon\varepsilon,\phi\phi\phi}p<0.001$.

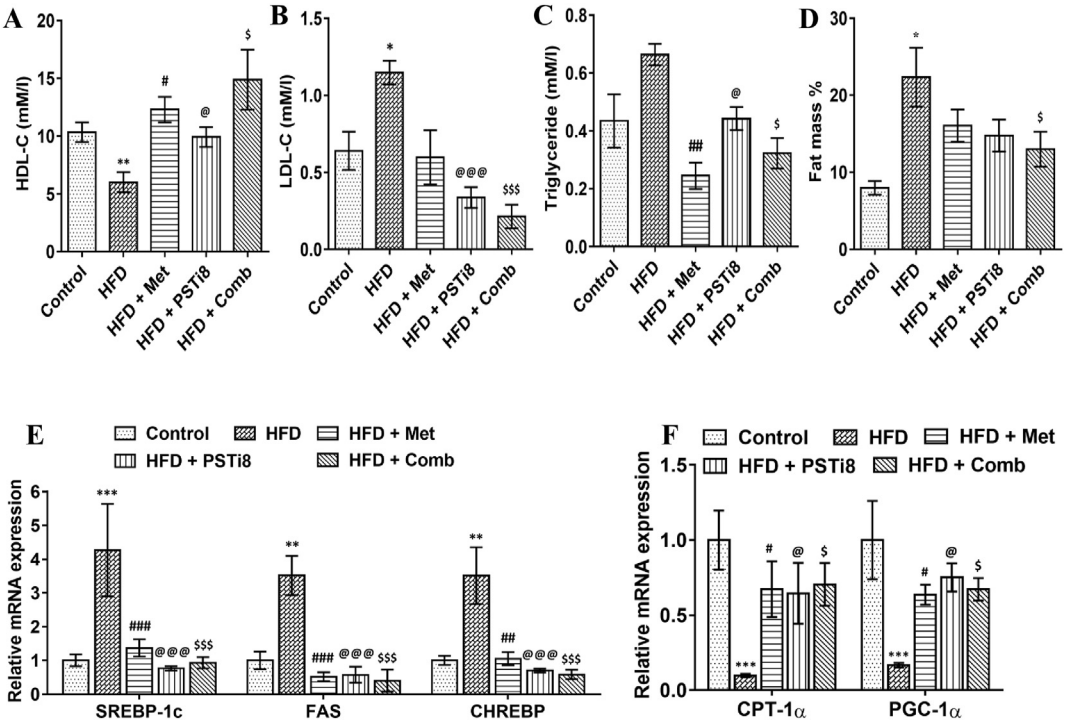

Figure 5. Effect of combination therapy on plasma lipid markers and unregulated lipid deposition plasma lipid markers (A) HDL-C, (B) LDL-C (C) Triglycerides were detected (n = 6). (D) Complete fat mass % was detected in body (n = 6). (E) Relative mRNA expression of lipogenic markers Srebp-1c, Fas, Chrebp and (B) important determinants of fatty acid oxidation Cpt-1α, Pgc-1α. Comparative significance for A–F represented as *, Control vs HFD; #, HFD vs HFD + Met; @, HFD vs HFD + PSTi8; $, HFD vs HFD + Comb. $^{*,\#,@,\$}p < 0.05$; $^{**,\#\#,@@,\$\$}p < 0.01$; $^{***,\#\#\#,@@@,\$\$\$}p < 0.001$.

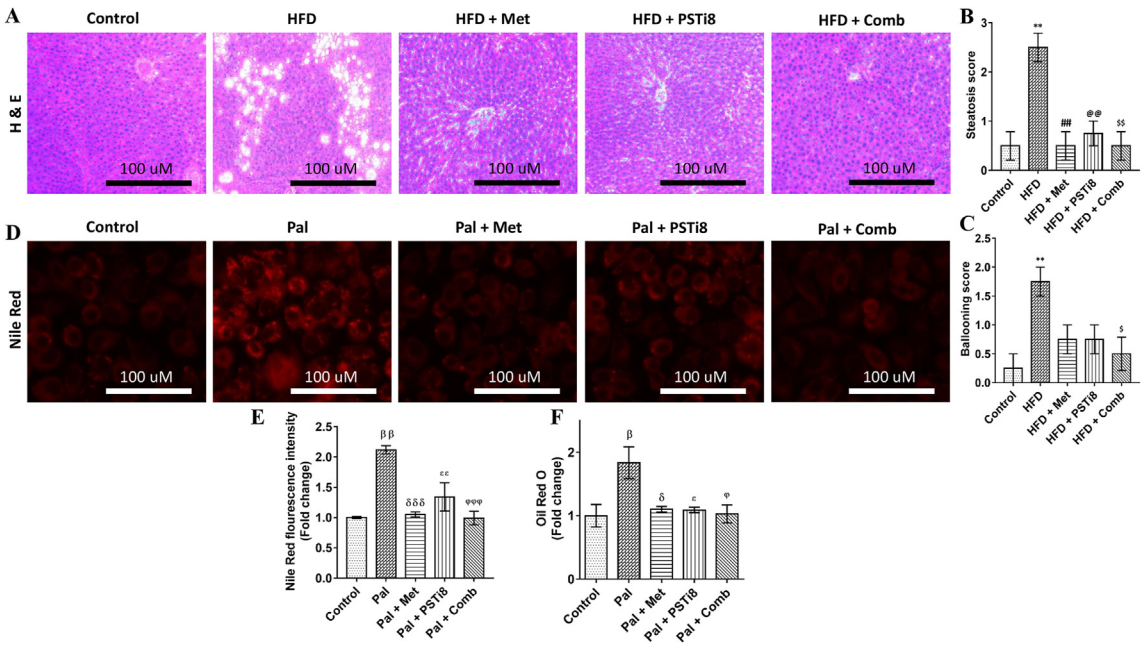

Figure 6. Combination therapy ameliorated lipid accumulation in the liver of HFD fed mice and insulin resistant HepG2 cells. We performed (A) H&E staining of liver sections that manifested presence of steatosis (B) and (C) ballooning in HFD fed group. (D) Nile Red staining, (E) its fluorescence intensity quantification and (F) Oil Red O staining displayed increased lipid accumulation in Pal treated HepG2 cells. Comparative significance for A–C and F, represented as *, Control vs HFD; #, HFD vs HFD + Met; @, HFD vs HFD + PSTi8; $, HFD vs HFD + Comb. $^{*, \#, @, \$}p < 0.05$; $^{**, \#\#, @@, \$\$}p < 0.01$; $^{***, \#\#\#, @@@, \$\$\$}p < 0.001$. For D–F, significance values depicted as $^{\beta,\delta,\varepsilon,\phi}p<0.05$; $^{\beta\beta,\delta\delta,\varepsilon\varepsilon,\phi\phi}p<0.01$; $^{\beta\beta\beta,\delta\delta\delta,\varepsilon\varepsilon\varepsilon,\phi\phi\phi}p<0.001$. Significance values represents $^{*, \#, @, \$}p < 0.05$; $^{**, \#\#, @@, \$\$}p < 0.01$; $^{***, \#\#\#, @@@, \$\$\$}p < 0.001$.

HFD group while increased in the HFD + Comb group. We also detected increased plasma levels of LDL-C (Figure 5B), triglycerides (Figure 5C) in the HFD group, and decreased the same in the HFD + Comb group. Fat mass percent was significantly reduced in HFD + Comb group (Figure 5D). We found increased expression of major transcriptional regulators of de-novo lipogeneses, such as Srebp-1c and its downstream regulatory gene Fas in the HFD group (Figure 5E). We also found increased expression of Chrebp (Figure 5E), which is mainly upregulated in response to carbohydrates and decreased the mRNA expression of genes promoting fatty acid oxidation, particularly Cpt-1α, and Pgc-1α (Figure 5F) in HFD group.

Furthermore, the effect of combination therapy on hepatic lipid accumulation was demonstrated by H & E staining of liver section and Nile Red and Oil Red O staining of HepG2 cells. We found enhanced steatosis and hepatic ballooning in HFD encountered mice but not in control (Figure 6A–C). Parallelly, the Pal exposed HepG2 cells exhibited increased fluorescence intensity of Nile Red (Figure 6D and E) and absorbance of Oil Red O (Figure 6F), which correspond to lipids aggregation in hepatocytes. Nonetheless, HFD mice kept on combination treatment unveiled protection from the aggravated extent of lipid accumulation.

3.5. Effect of combination therapy on the hepatic gluconeogenesis and inflammation

To detect the disruption of insulin suppressive effects on hepatic gluconeogenesis, we distinguished the relative mRNA expression of essential regulatory genes of gluconeogenesis. Relative mRNA of Pepck and G6pse was found to be increased in HFD group and significantly reduced in HFD + Comb group (Figure 7A). Next, we detected the hepatic expression of proinflammatory markers. It has been reported previously that higher Fetuin-A expression stimulates the expression of proinflammatory markers during compromised insulin release. We investigated relative mRNA expression of TNF-α, IL-6, IL-1β by RT-PCR and found enhanced expression of TNF-α, IL-6, IL-1β (Figure 7B) in HFD group while expression was mitigated significantly for the same in HFD + Comb group. In compliance with these results, these results revealed the involvement of hepatic gluconeogenesis while prevailing IR in HFD mice, which manifests augmented fasting blood glucose due to increased hepatic glucose disposal. Accordingly, Combination therapy efficiently improved hepatic gluconeogenesis, reduced Fetuin-A instigated proinflammatory markers, and thereby helps in reducing inflammatory milieu and improving related comorbidities in T2D.

3.6. Evaluation of metabolic energy homeostasis

Evaluation of metabolic characteristics associated with energy expenditure may provide an awaited investigation of switching between carbohydrate and fat metabolism following Met and PSTi8 administration alone and in combination during the superfluous nutritional environment. We detected VO2 consumption (Figure 8A, F), VCO2 production (Figure 8B, G), RER (Figure 8C and H), heat production (Figure 8D and I) and X-axis movement (Figure E and J) during light and dark period (24h). We found a significant increase in VO2, VCO2, and RER (Figure 8A–C), while heat production was not much affected. These results suggest that increased RER may indicate enhanced metabolic flexibility and increased carbohydrate oxidation to fulfill energy requirements.

4. Discussion

Glucose intolerance and IR are the major predecessors of T2D. Previous studies reported that HFD induces IR initially by hyperinsulinemia to counterbalance the complete or partial loss of insulin at the expense of increased lipogenesis and gluconeogenesis (Pories and Dohm, 2012). On the contrary, fatty acids are also delineated to cause IR due to attenuated

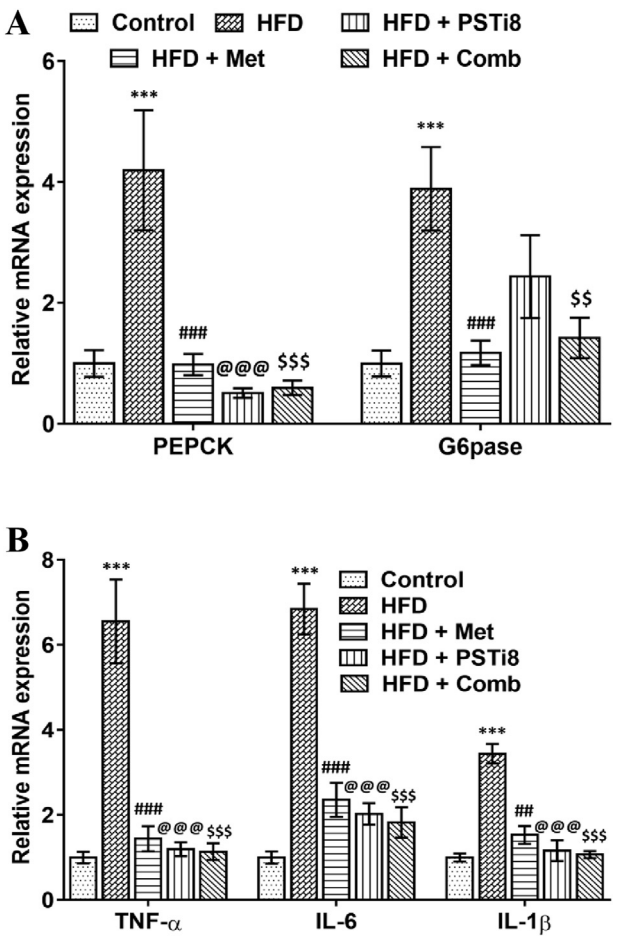

Figure 7. Combination therapy ameliorates glucose metabolism and expression of proinflammatory markers in liver (A) Relative mRNA levels of Pepck and G6pase were studied by qRT-PCR (n = 6). (B) Relative mRNA expression of Tnf-α, Il-6, Il-1β in liver (n = 6). Results represented as means ± SEM. Significance for Comparison among groups was represented as *, Control vs HFD; #, HFD vs HFD + Met; @, HFD vs HFD + PSTi8; $, HFD vs HFD + Comb. $^{*, \#, @, \$}p < 0.05$; $^{**, \#\#, @@, \$\$}p < 0.01$; $^{***, \#\#\#, @@@, \$\$\$}p < 0.001$.

hepatic insulin clearance (Kissebah and Peiris, 1989). Foregoing studies have reported that Met monotherapy requires additional second-line therapy (Kumar, 2012) due to gastrointestinal intolerance associated with the Met and progressive nature of diabetes. PST is an endogenous peptide known to have adverse effects on insulin secretion (Tatemoto et al., 1986) and causes metabolic deregulation by increasing NEFA in circulation (Gupta et al., 2020). Increased PST levels were detected in diabetic patients (Funakoshi et al., 1990; Kim et al., 2010). PSTi8 is a well elucidated potential inhibitor of endogenous peptide PST, as we mentioned in our previous studies (Gupta et al., 2019; Valicherla et al., 2019). Above all, we optimized the Met and PSti8 doses in combination for further *in-vitro* and *in-vivo* studies and found that Met 50 μM and PSTi8 100 nM is best possible combination in order to use in *in-vitro* experiments while Met 150 mg/kg with PSTi8 2.5 mg/kg combination worked best among other combination doses during acute treatment (Figure 2A–E) in HFD induced diabetic mice. Considering these aspects, we were intended to speculate implications of combination therapy of Met and PSTi8, at their half of therapeutic dosage, used in preceding studies (Hossain et al., 2018; Tajima et al., 2011). Accordingly, we observed that HFD resulted in minimal alterations in the bodyweight while gradually increased FBG, IR, and impaired insulin response (Figure 2F and G). These outcomes were also in accordance with the previously mentioned study where blood glucose, insulin level, and also triglycerides were found to be enhanced in the HFD diabetic mice model (Wu et al., 2009). Upon lipid overload, HFD mice displayed reduced glucose disposal, mitigated insulin-induced suppression of blood glucose due to increased insulin insensitivity. HFD + Comb group effectually revealed significant improvement in glucose tolerance and insulin sensitivity (Figure 2H–O), corrected FBG, more efficiently.

It was previously explored that HFD causes an increase in the PST level, which leads to enhanced NEFA (Gupta et al., 2020), which may further promote the activation of Fetuin-A. Fetuin-A, a hepatokine synthesized by the liver, induces IR (Ix et al., 2008; Stefan et al., 2008) and inflammation (Boden et al., 2005). It must be mentioned that we found increased plasma concentration of PST and NEFA (Figure 3) in HFD mice (Figure 3A), which drove us to examine the Fetuin-A level in the circulation and liver. We found enhanced plasma Fetuin-A and also increased expression at mRNA and protein (Figure 3C–E) level in disease conditions (HFD). Combination therapy of Met and PSTi8 attenuated the expression of Fetuin-A, which ultimately leads to reduced Fetuin-A plasma level. In support of these findings, we also investigated Fetuin-A in Pal-induced insulin-resistant HepG2 cells by immunofluorescence. Increased fluorescence intensity was found in insulin-resistant HepG2 cells, while combination therapy reduced Fetuin-A fluorescence intensity (Figure 3F and G). This improvement in the Fetuin-A level would possibly be related to improved insulin secretion and insulin sensitivity, as depicted in Figure 4. We also found that combination therapy significantly increased glycogen production in the liver (Figure 4C), manifested improved insulin response. It was previously reported that Pal (0.25 mM) might lead to the development of IR (Gao et al., 2010), which can be an ideal model to examine insulin sensitization impact. Interestingly, combination therapy significantly reduced glucose production in Pal induced insulin-resistant HepG2 cells (Figure 4D). IRS and AKT are chief downstream regulatory elements of insulin signaling where inhibitory phosphorylation of IRS (Ser-307) and activating phosphorylation of AKT (Ser-473) provides essential information about the progression of IR and diabetes (Saltiel and Kahn, 2001). Expectedly in agreement with the former findings, in the liver, we detected increased p-IRS (Ser-307) and decreased p-AKT (Ser-473) in HFD mice. Combination therapy attenuated the expression of p-IRS (Ser-307) and enhanced p-AKT (Ser-473) (Figure 4E, F) expression, which distinctly stated that improved insulin sensitivity allied with improved hepatic insulin signaling. Previous researchers asserted the evolution of alterations in lipid and carbohydrate metabolism in the HFD model (Nath et al., 2017). In line with previous findings, we found decreased HDL, increased level of LDL, and triglycerides in plasma of HFD mice while combination therapy significantly increased plasma HDL level, decreased plasma LDL and triglycerides (Figure 5A–C). This improved lipid profile resulted in a more significant reduction in body fat mass percent (Figure 5D) with combination therapy, than Met and PSTi8 alone. HFD induced IR leads to dysregulated lipid signaling following enhanced fatty acid synthesis (Brown and Goldstein, 2008). Srebp-1c gets overactivated in response to compensatory hyperinsulinemia during lipid overburden (Moon et al., 2012). Intriguingly, enhanced expression of hepatic Srebp-1c was observed in HFD mice and combination therapy remarkably attenuated expression (Figure 5E) of Srebp-1c, a master regulator of de-novo lipogenesis. Furthermore, regulatory transcriptional factors of lipogenesis Fas, Chrebp were also found to be attenuated significantly in (Figure 5E) HFD + Comb group equivalent to alone Met and PSTi8. Conversely, important markers of fatty acid oxidation CPT-1α, PGC-1α were found to be increased (Figure 5F). These results indicated that HFD caused detrimental effects on lipid metabolism while combination therapy effectively worked towards utilization of fat deposited in liver.

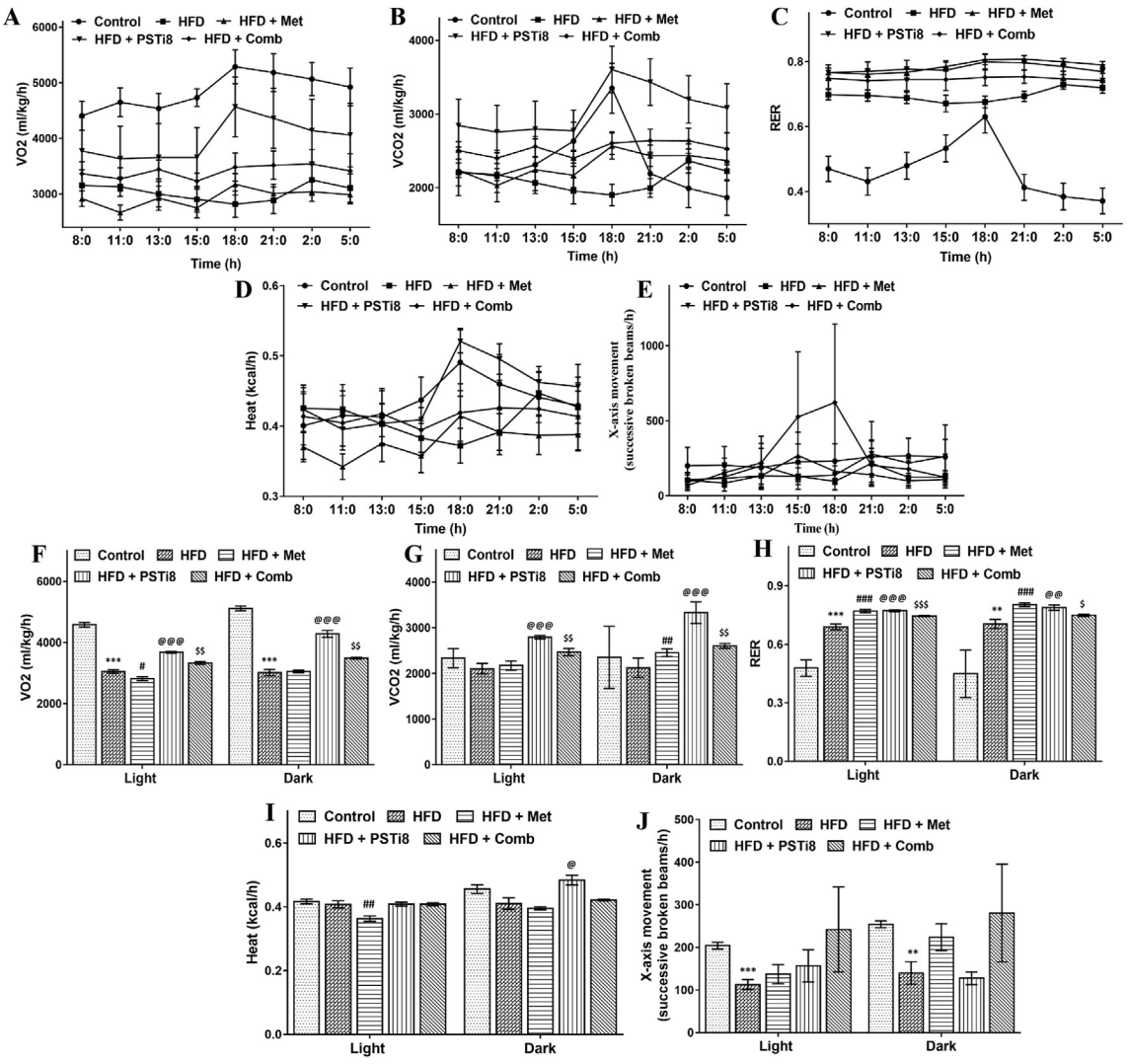

Figure 8. Effect of Combination therapy on energy homeostasis – Study of metabolic parameters (24 h) in HFD mice may lead to emergence of new approaches regarding the consumption of metabolic fuel. Metabolic parameters (A, F) VO2 (mL/kg/h); (B, G) VCO2 (mL/kg/h); (C, H) RER (VCO2/VO2); (D, I) Heat production; (E, J) X-axis movement, were assessed in comprehensive lab animal monitoring system (CLAMS). Results obtained were shown as means ± SEM (n = 5). Significance comparison was represented as *, Control vs HFD; #, HFD vs HFD + Met; @, HFD vs HFD + PSTi8; $, HFD vs HFD + Comb. $^{*,\#,@,\$}p < 0.05$; $^{**,\#\#,@@,\$\$}p < 0.01$; $^{***,\#\#\#,@@@,\$\$\$}p < 0.001$.

These findings led us to explore the effect of the combination on lipid accumulation in liver and Pal-induced insulin-resistant HepG2 cells. H & E staining and histological score analysis revealed steatosis and ballooning in the liver of HFD mice (Figure 6A–C). Nevertheless, combination therapy noticeably reduced ectopic lipid accumulation in the liver as demonstrated by H & E staining with improved tissue architecture and fewer lipid droplets formation. It must be mentioned that the combination therapy of Met and PSTi8 efficiently reduced lipid droplets formation in insulin-resistant HepG2 cells as determined by Oil Red O and Nile Red staining (Figure 6D–F).

It was also suggested that overnutrition caused by HFD, gives rise to inflammation, and increased gluconeogenesis (Lackey and Olefsky, 2016). In this regard, we identified increased expression of Pepck and G6pase, important regulators of gluconeogenesis, and significantly reduced expression of these genes (Figure 7A) in HFD + Comb group. Furthermore, the expression of proinflammatory markers is intriguingly associated with increased fat accumulation in the liver and the progression of IR (van der Heijden et al., 2015). Results displayed elevated expression of proinflammatory markers TNF-α, IL-6, and IL-1β in the liver of HFD mice. Contrarily, combination therapy significantly reduced the expression of these markers (Figure 7B). These results revealed that combination therapy might diminish lipid overload by attenuating lipogenesis and increasing fat oxidation, which may be responsible for reduced expression of Fetuin-A and proinflammatory markers. It must be considered here that we found increased gluconeogenesis and lipogenesis in the HFD group, which would be a reasonable indication of IR due to which insulin promotes lipogenesis and loses its control over gluconeogenesis (Brown and Goldstein, 2008; Honma et al., 2018).

Previous studies showed that reduced physical activity and oxygen consumption are associated with diabetes (Gürdal et al., 2015). Accordingly, we found less movement and decreased oxygen consumption in HFD mice, whereas, mice treated with combination treatment showed increased activity and significantly increased oxygen

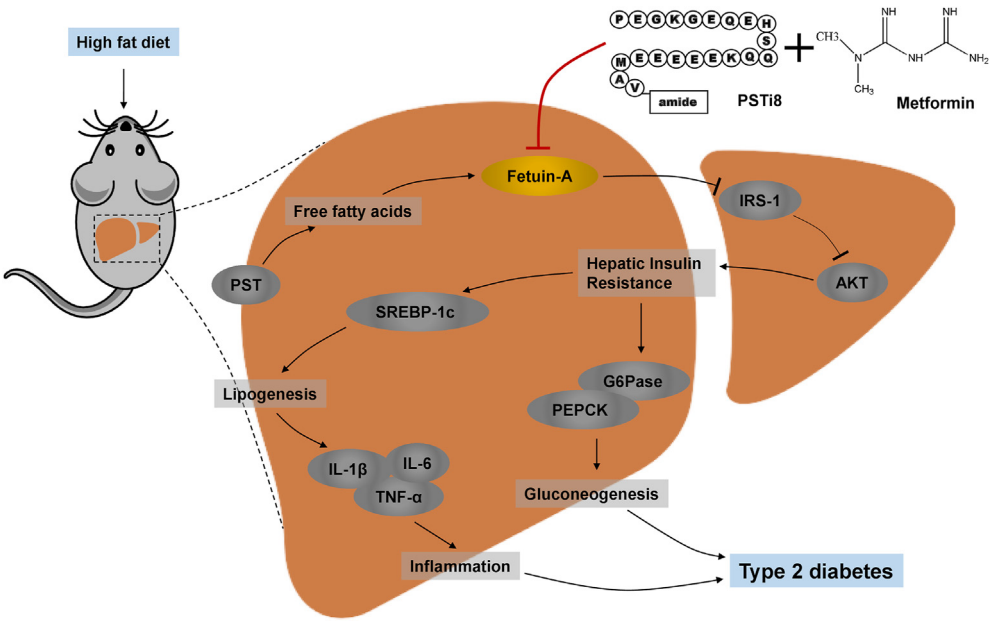

Figure 9. Combination of Met and PSTi8 (at reduced therapeutic regimen) protects from T2D by inhibiting hepatic Fetuin-A and associated IR subsequently precludes comorbidities particularly lipogenesis, gluconeogenesis and inflammation in liver.

consumption. Additionally, combination therapy promoted RER. One plausible explanation might be that HFD animals have lost their capacity to oxidize carbohydrates efficiently as compared to control animals, while combination therapy reverses this abnormality (Figure 8).

5. Conclusion

In conclusion, the combination approach of Met and PSTi8 may work as a potential therapy to reverse Fetuin-A mediated IR, including its associated risk elements at reduced therapeutic doses of Met and PSTi8 (Figure 9). The current findings may fill gaps in our understanding of the pathogenesis of T2D, which may further assist in the development of new perceptions towards the advent of novel measures of diabetes prevention, management, and treatment.

Declarations

Author contribution statement

J.R. Gayen: Conceived and designed the experiments; Analyzed and interpreted the data; Contributed reagents, materials, analysis tools or data; Wrote the paper.

P. Singh: Conceived and designed the experiments; Performed the experiments; Analyzed and interpreted the data; Wrote the paper.

R. Garg, U.K. Goand, M. Riyazuddin, M.I. Reza, A. A. Syed, A.P. Gupta and A. Husain: Performed the experiments; Analyzed and interpreted the data.

Funding statement

P. Singh was supported by University Grants Commission. CSIR, Govt. of India. J.R. Gayen was supported by CSIR, Govt. of India and Department of Biotechnology, Govt. of India (CSIR-CDRI communication number for this article is 10125).

Competing interest statement

The authors declare no conflict of interest.

Additional information

No additional information is available for this paper.

References

Ables, G.P., Perrone, C.E., Orentreich, D., Orentreich, N., 2012. Methionine-restricted C57BL/6J mice are resistant to diet-induced obesity and insulin resistance but have low bone density. PloS One 7.

Arulmozhi, D.K., Kurian, R., Bodhankar, S.L., Veeranjaneyulu, A., 2008. Metabolic effects of various antidiabetic and hypolipidaemic agents on a high-fat diet and multiple low-dose streptozocin (MLDS) mouse model of diabetes. J. Pharm. Pharmacol. 60, 1167–1173.

Bandyopadhyay, G.K., Lu, M., Avolio, E., Siddiqui, J.A., Gayen, J.R., Wollam, J., Vu, C.U., Chi, N.-W., O'Connor, D.T., Mahata, S.K., 2015. Pancreastatin-dependent inflammatory signaling mediates obesity-induced insulin resistance. Diabetes 64, 104–116.

Benarbia, M. el A., Macherel, D., Faure, S., Jacques, C., Andriantsitohaina, R., Malthièry, Y., 2013. Plasmatic concentration of organochlorine lindane acts as metabolic disruptors in HepG2 liver cell line by inducing mitochondrial disorder. Toxicol. Appl. Pharmacol. 272, 325–334.

Boden, G., She, P., Mozzoli, M., Cheung, P., Gumireddy, K., Reddy, P., Xiang, X., Luo, Z., Ruderman, N., 2005. Free fatty acids produce insulin resistance and activate the proinflammatory nuclear factor-κB pathway in rat liver. Diabetes 54, 3458–3465.

Brown, M.S., Goldstein, J.L., 2008. Selective versus total insulin resistance: a pathogenic paradox. Cell Metabol. 7, 95–96.

Calixto, M.C., Lintomen, L., André, D.M., Leiria, L.O., Ferreira, D., Lellis-Santos, C., Anhê, G.F., Bordin, S., Landgraf, R.G., Antunes, E., 2013. Metformin attenuates the exacerbation of the allergic eosinophilic inflammation in high fat-diet-induced obesity in mice. PloS One 8.

Cao, J., Meng, S., Chang, E., Beckwith-Fickas, K., Xiong, L., Cole, R.N., Radovick, S., Wondisford, F.E., He, L., 2014. Low concentrations of metformin suppress glucose production in hepatocytes through AMP-activated protein kinase (AMPK). J. Biol. Chem. 289, 20435–20446.

Funakoshi, A., Tateishi, K., Shinozaki, H., Matsumoto, M., Wakasugi, H., 1990. Elevated plasma levels of pancreastatin (PST) in patients with non-insulin-dependent diabetes mellitus (NIDDM). Regul. Pept. 30, 159–164.

Gao, D., Nong, S., Huang, X., Lu, Y., Zhao, H., Lin, Y., Man, Y., Wang, S., Yang, J., Li, J., 2010. The effects of palmitate on hepatic insulin resistance are mediated by NADPH Oxidase 3-derived reactive oxygen species through JNK and p38MAPK pathways. J. Biol. Chem. 285, 29965–29973.

Gayen, J.R., Saberi, M., Schenk, S., Biswas, N., Vaingankar, S.M., Cheung, W.W., Najjar, S.M., O'Connor, D.T., Bandyopadhyay, G., Mahata, S.K., 2009. A novel pathway of insulin sensitivity in chromogranin A null mice a crucial role for pancreastatin in glucose homeostasis. J. Biol. Chem. 284, 28498–28509.

Guo, S., 2014. Insulin signaling, resistance, and the metabolic syndrome: insights from mouse models to disease mechanisms. J. Endocrinol. 220, T1.

Gupta, A.P., Garg, R., Singh, P., Goand, U.K., Syed, A.A., Valicherla, G.R., Riyazuddin, M., Mugale, M.N., Gayen, J.R., 2020. Pancreastatin inhibitor PSTi8 protects the obesity associated skeletal muscle insulin resistance in diet induced streptozotocin-treated diabetic mice. Eur. J. Pharmacol. 173204.

Gupta, A.P., Singh, P., Garg, R., Valicherla, G.R., Riyazuddin, M., Syed, A.A., Hossain, Z., Gayen, J.R., 2019. Pancreastatin inhibitor activates AMPK pathway via GRP78 and ameliorates dexamethasone induced fatty liver disease in C57BL/6 mice. Biomed. Pharmacother. 116, 108959.

Gürdal, A., Kasikcioglu, E., Yakal, S., Bugra, Z., 2015. Impact of diabetes and diastolic dysfunction on exercise capacity in normotensive patients without coronary artery disease. Diabetes Vasc. Dis. Res. 12, 181–188.

Honma, M., Sawada, S., Ueno, Y., Murakami, K., Yamada, T., Gao, J., Kodama, S., Izumi, T., Takahashi, K., Tsukita, S., 2018. Selective insulin resistance with differential expressions of IRS-1 and IRS-2 in human NAFLD livers. Int. J. Obes. 42, 1544–1555.

Hossain, Z., Valicherla, G.R., Gupta, A.P., Syed, A.A., Riyazuddin, M., Chandra, S., Siddiqi, M.I., Gayen, J.R., 2018. Discovery of pancreastatin inhibitor PSTi8 for the treatment of insulin resistance and diabetes: studies in rodent models of diabetes mellitus. Sci. Rep. 8, 8715.

Ix, J.H., Wassel, C.L., Kanaya, A.M., Vittinghoff, E., Johnson, K.C., Koster, A., Cauley, J.A., Harris, T.B., Cummings, S.R., Shlipak, M.G., 2008. Fetuin-A and incident diabetes mellitus in older persons. Jama 300, 182–188.

Kim, D.-S., Jeong, S.-K., Kim, H.-R., Kim, D.-S., Chae, S.-W., Chae, H.-J., 2010. Metformin regulates palmitate-induced apoptosis and ER stress response in HepG2 liver cells. Immunopharmacol. Immunotoxicol. 32, 251–257.

Kissebah, A.H., Peiris, A.N., 1989. Biology of regional body fat distribution: relationship to non-insulin-dependent diabetes mellitus. Diabetes Metab. Rev. 5, 83–109.

Kumar, A., 2012. Second line therapy: type 2 diabetic subjects failing on metformin GLP-1/DPP-IV inhibitors versus sulphonylurea/insulin: for GLP-1/DPP-IV inhibitors. Diabetes. Metab. Res. Rev. 28, 21–25.

Lackey, D.E., Olefsky, J.M., 2016. Regulation of metabolism by the innate immune system. Nat. Rev. Endocrinol. 12, 15.

Luo, J., Quan, J., Tsai, J., Hobensack, C.K., Sullivan, C., Hector, R., Reaven, G.M., 1998. Nongenetic mouse models of non—insulin-dependent diabetes mellitus. Metab. Exp. 47, 663–668.

Moon, Y.-A., Liang, G., Xie, X., Frank-Kamenetsky, M., Fitzgerald, K., Koteliansky, V., Brown, M.S., Goldstein, J.L., Horton, J.D., 2012. The Scap/SREBP pathway is essential for developing diabetic fatty liver and carbohydrate-induced hypertriglyceridemia in animals. Cell Metabol. 15, 240–246.

Nath, S., Ghosh, S.K., Choudhury, Y., 2017. A murine model of type 2 diabetes mellitus developed using a combination of high fat diet and multiple low doses of streptozotocin treatment mimics the metabolic characteristics of type 2 diabetes mellitus in humans. J. Pharmacol. Toxicol. Methods 84, 20–30.

Olefsky, J.M., 1990. The insulin receptor: a multifunctional protein. Diabetes 39, 1009–1016.

Pories, W.J., Dohm, G.L., 2012. Diabetes: have we got it all wrong?: hyperinsulinism as the culprit: surgery provides the evidence. Diabetes Care 35, 2438–2442.

Reaven, G.M., 1988. Role of insulin resistance in human disease. Diabetes 37, 1595–1607.

Rena, G., Hardie, D.G., Pearson, E.R., 2017. The mechanisms of action of metformin. Diabetologia 60, 1577–1585.

Saeedi, P., Petersohn, I., Salpea, P., Malanda, B., Karuranga, S., Unwin, N., Colagiuri, S., Guariguata, L., Motala, A.A., Ogurtsova, K., 2019. Global and regional diabetes prevalence estimates for 2019 and projections for 2030 and 2045: results from the international diabetes federation diabetes atlas. Diabetes Res. Clin. Pract. 157, 107843.

Salomäki, H., Vähätalo, L.H., Laurila, K., Jäppinen, N.T., Penttinen, A.-M., Ailanen, L., Ilyasizadeh, J., Pesonen, U., Koulu, M., 2013. Prenatal metformin exposure in mice programs the metabolic phenotype of the offspring during a high fat diet at adulthood. PloS One 8.

Saltiel, A.R., Kahn, C.R., 2001. Insulin signalling and the regulation of glucose and lipid metabolism. Nature 414, 799–806.

Seppala-Lindroos, A., Vehkavaara, S., Häkkinen, A.-M., Goto, T., Westerbacka, J., Sovijärvi, A., Halavaara, J., Yki-Järvinen, H., 2002. Fat accumulation in the liver is associated with defects in insulin suppression of glucose production and serum free fatty acids independent of obesity in normal men. J. Clin. Endocrinol. Metab. 87, 3023–3028.

Stefan, N., Fritsche, A., Weikert, C., Boeing, H., Joost, H.-G., Häring, H.-U., Schulze, M.B., 2008. Plasma fetuin-A levels and the risk of type 2 diabetes. Diabetes 57, 2762–2767.

Syed, A.A., Reza, M.I., Shafiq, M., Kumariya, S., Singh, P., Husain, A., Hanif, K., Gayen, J.R., 2020. Naringin ameliorates type 2 diabetes mellitus-induced steatohepatitis by inhibiting RAGE/NF-κB mediated mitochondrial apoptosis. Life Sci. 257, 118118.

Tajima, A., Hirata, T., Taniguchi, K., Kondo, Y., Kato, S., Saito-Hori, M., Ishimoto, T., Yamamoto, K., 2011. Combination of TS-021 with metformin improves hyperglycemia and synergistically increases pancreatic β-cell mass in a mouse model of type 2 diabetes. Life Sci. 89, 662–670.

Tatemoto, K., Efendić, S., Mutt, V., Makk, G., Feistner, G.J., Barchas, J.D., 1986. Pancreastatin, a novel pancreatic peptide that inhibits insulin secretion. Nature 324, 476–478.

Un Nisa, K., Reza, M.I., 2019. Key relevance of epigenetic programming of adiponectin gene in pathogenesis of metabolic disorders. Endocr. Metab. Immune Disord. - Drug Targets.

Valicherla, G.R., Gupta, A.P., Hossain, Z., Riyazuddin, M., Syed, A.A., Husain, A., Lahiri, S., Dave, K.M., Gayen, J.R., 2019. Pancreastatin inhibitor, PSTi8 ameliorates metabolic health by modulating AKT/GSK-3β and PKCλ/ζ/SREBP1c pathways in high fat diet induced insulin resistance in peri-/post-menopausal rats. Peptides 120, 170147.

van der Heijden, R.A., Sheedfar, F., Morrison, M.C., Hommelberg, P.P.H., Kor, D., Kloosterhuis, N.J., Gruben, N., Youssef, S.A., de Bruin, A., Hofker, M.H., 2015. High-fat diet induced obesity primes inflammation in adipose tissue prior to liver in C57BL/6j mice. Aging (Albany NY) 7, 256.

Wu, S., Wang, G., Liu, Z., Rao, J., Lü, L., Xu, W., Wu, S., Zhang, J., 2009. Effect of geniposide, a hypoglycemic glucoside, on hepatic regulating enzymes in diabetic mice induced by a high-fat diet and streptozotocin. Acta Pharmacol. Sin. 30, 202–208.

Xiao, Q., Zhang, S., Yang, C., Du, R., Zhao, J., Li, J., Xu, Y., Qin, Y., Gao, Y., Huang, W., 2019. Ginsenoside Rg1 ameliorates palmitic acid-induced hepatic steatosis and inflammation in HepG2 cells via the AMPK/NF-B pathway. Internet J. Endocrinol. 2019.